JOURNAL OF MARITIME RESEARCH

Vol XXI. No. II (2024) pp 317–325

ISSN: 1697-4840, www.jmr.unican.es

A Simulation Study on the Performance of Jacket Type Offshore Structures Using Machine Learning Algorithms

Engin Gücüyen[1,*], Aybike Özyüksel Çiftçioğlu[2], R. Tuğrul Erdem[3]

ARTICLE INFO

Article history:
Received 22 Jan 2024;
in revised from 03 Feb 2024;
accepted 26 Mar 2024.

Keywords:
Machine learning; Marine environment; Numerical analysis, Offshore structure; Xgboost regressor.

ABSTRACT

In this study, the behaviors of jacket-type offshore structures are numerically investigated. The examined four-legged models with a total height of 60 m have four layers and three different cylindrical element sizes are fixed to the seabed. The structures are under the effect of environmental forces, including wind and wave loads, as well as operational loads. Three different marine environments have been generated in environmental modeling. Thus, the parametric study has been performed using bidirectional fluid-structure interaction (FSI) analyses of 36 models. Structural outputs such as displacement, reaction force, and stress values are determined by numerical analyses. In the second part of the study, the implementation of machine learning algorithms, including Xgboost, Random Forest, and Support Vector regressors, is employed to automate the assessment of performance in jacket-type offshore structures. The evaluation of these machine learning models in predicting the displacement, reaction force, and stress values of offshore jacket structures is conducted, revealing Xgboost as the most promising technique, although with satisfactory overall performance across all algorithms. These findings provide empirical evidence supporting the feasibility and applicability of employing machine learning methodologies in the analysis of performance for jacket-type offshore structures.

1. Introduction.

In the present era, jacket-type offshore structures predominantly function as essential components of energy facilities. Construction in each type of soil and depth, availability of installation vessels and driven equipment, and being light are some advantages of these structures.

These advantages enable offshore structures to be preferred over single pile, multiple piles, and suction caisson types (Zhang et al. 2020, Xie et al 2021).Although jacket-type offshore structures have such advantages, the construction of jacket structures is more difficult for those on land, due to adverse environmental situations, including wave-wind conditions and difficulties in assembly and disassembling (Mousavi et al. 2023).

Performing maintenance and remedial operations on offshore jacket structures poses significant challenges, occasionally bordering on infeasibility, thereby emphasizing the imperative for rigorous safety protocols. In this context, the acquisition of data, along with elucidating the source and fundamental nature of the amassed data within a system, assumes paramount importance (Liu, Hajj and Bao, 2022). The data collection process can be carried out with artificial and real data. Experimental and numerical studies may be performed to obtain real data. With increasing resources of data and computing power resources from time to time, traditional methods such as numerical and experimental techniques are being replaced by artificial intelligence (Lin et al. 2022).

Numerical solutions can be used for training the artificial models as used in the study of (Zhang and Zhao 2022). In this work, CFD simulations are used as machine-learning models

[1]Professor of Civil Engineering Department of Manisa Celal Bayar University, Turkey.
[2]Assistant Professor of Civil Engineering Department of Manisa Celal Bayar University, Turkey.
[3]Professor of Civil Engineering Department of Manisa Celal Bayar University, Turkey.
[*]Corresponding author: E. Gücüyen, Tel. (+090) 2362012321. E-mail Address: engin.gucuyen@cbu.edu.tr.

of a novel wake. By learning from the CFD model through flow field data, the machine learning model generalizes well to unknown flow scenarios and learns the qualitative features of wind turbine wake flows successfully. The mixed finite element method is employed by (Ferreira et al. 2022) to generate the input data set of fluid flow fractured porous media. As output, the generative adversarial networks model predicts the pressure inside the fracture. Similarly, the training data of structural deformation of a deck plate is supplied from a nonlinear buckling finite element method in the study of (Oh et al. 2021), neural network-based generative adversarial network model successfully predicted the distortion with high accuracy value. In all three studies, it has been stated that the estimation time is on the order of seconds.

Parametric studies by finite element methods have also been performed in the literature. In the study of (Zhang et al. 2020), different types of brace are modeled to investigate brace type on the bearing capacity and load transfer mode of offshore jacket structures. The numerical studies are carried out by the finite element software ABAQUS. Besides, the effect of story number and floor plan on the modal behavior is examined. Another study has investigated the effect of brace types (Tran, Kim and Lee 2022). The new three-legged jacket-type structures with three various bracing topological forms are developed based on the external diameters and superstructure mass of existing four-legged jackets. Different loading directionality effects are also investigated by twelve different design load cases. The best performance among the bracing systems has been detected in the end. In the other study by the same authors (Tran, and Lee, 2022), the lowest material costs of the four different depths of bracing types in two different water are investigated by applying the same load effects (Tran, Kim and Lee 2022). In the study of (Jalbi and Bhattacharya, 2020), the effects of structural properties, environmental forces, and soil characteristics on the design procedures of the offshore jacket structure are examined. For this purpose, the parametric study is performed for varying wind velocity, water depth, weight of the superstructure, and soil types to reveal the concept design of the structure. Structural behaviors of three jacket-type offshore structures are compared under regular and irregular wave-loading conditions (Wei, Myers and Arwade, 2017). The reference model, stiffer model than the reference model, and more flexible model than the stiffer model constitute three jacket models. The other parametric studies investigating the numerical behavior of offshore jackets can be given as (Chen et al 2016, Bagheri and Kim, 2016, Abhinav and Nilanjan, 2019, Lu et al 2019).

To estimate the dynamic response of offshore structures under environmental loads, fluid-structure (FSI) methods are commonly used to investigate the dynamic behavior of structures. FSI analyses coupling attributes are classified as one-way and two-way. Finite element analysis is employed for both examinations. Finite elements supported by FSI analysis can be generated by either the Eulerian technique (Martínez et al. 2009) or the Lagrangian technique (Gücüyen, Erdem and Gökkuş, 2016). In addition, both techniques can be used in Arbitrary Lagrangian Eulerian (ALE) (Korobenko et al. 2017, Liu, 2016.) and Coupled Eulerian-Lagrangian (CEL) (Gücüyen et al. 2020) analyses. Abaqus finite element program is widely used by researchers for interaction modeling (ABAQUS User's Manual, 2015).

Although FSI-aided parametric studies have been performed about the effect of layer numbers and section geometries on offshore jackets, there are few studies about CEL-based two-way FSI analyses in the literature. In this study, three-dimensional finite-element models of the structures and surroundings are modeled within the framework (ABAQUS/CAE) via CEL analysis. In the first part of the study; displacement, reaction force, and Von-Mises stress values of the section geometries have been determined for different environmental load effects.

Artificial intelligence (AI) is a broad term that encompasses many different types of technology. It is a branch of computer science that develops intelligent systems that are able to perform tasks usually done by humans (Khalilpourazari et al. 2021, Khalilpourazari and Pasandideh, 2021). Machine learning is a subset of AI that allows computers to learn from data without being programmed in advance. It has the ability for a computer program to automatically improve its performance on a given task by analyzing past performance. In order for machine learning to work, there needs to be an input dataset with enough information for the algorithm to learn from. The algorithm then goes through this dataset and tries different methods until it finds one that works best for the given problem. Machine learning algorithms can be applied to any task where there is a set of features (inputs) and desired labels (outputs). There are a lot of machine learning algorithms in the literature that can be applied to any type of problem where prediction or decision-making under uncertainty is required: Xgboost, Random Forest, Support Vector, etc. (Özyüksel and Naser, 2022, Naser, 2021).

Random Forest is a type of supervised machine learning algorithm that uses a large collection of decision trees to model complex relationships between variables. It is a powerful algorithm that can make accurate predictions on the basis of limited data. The main goal of Random Forest is to create a decision tree from an input dataset, which can be used for classification or regression analysis. Random Forest uses an ensemble method for creating decision trees, where it takes multiple decision trees created from different subsets of data as inputs and combines them into one final tree with higher accuracy than any individual tree would have achieved by itself. It can be used to predict continuous outcomes or categorical outcomes. It has been widely used in the fields of machine learning, prediction modeling, text analytics, data mining, and bioinformatics (Breiman, 2021).

Extreme Gradient Boosting (Xgboost) is a gradient-boosting machine learning algorithm that can be applied in a wide range of fields. It is an open-source library that aims to solve large-scale regression problems. It can be used for classification and regression and has the ability to make predictions using different types of features. It works by iteratively building models with different parameters, which makes it suitable for both small and large datasets. It has been widely adopted in the field of data science and has been applied to many problems such as time series, text analysis, natural language processing, and

machine learning (Chen and Guestrin, 2016).

The support vector regressor is a machine-learning algorithm that is used for classification and regression problems. It is a nonparametric technique that uses a kernel function to fit a regression model. The kernel function is one of the most important elements in support vector regression. A kernel function can be used to reduce the dimensionality of data sets, which makes it easier for the algorithm to find a solution. The support vector regressor has been extensively applied in the field of computer vision and artificial intelligence. It has been widely used in many fields including image processing, natural language processing, bioinformatics, statistics, etc (Quinlan, 1986).

In the second part of the study, machine learning automates how jacket-type offshore structures perform by using prior experience and statistical data to forecast the future performance of these structures in different environmental load effects. Xgboost, Random Forest, and Support Vector regression algorithms are implemented to carry out the analyses. The results show that the jacket-type offshore structure can be effectively analyzed using the machine learning algorithms presented in this study and that these models are both reliable and effective. With continued advances in machine learning, these findings show a promising direction for predicting the behavior of jackets based on Abaqus outcomes.

2. Structural Models and Environmental Conditions.

In the structural modeling phase of the study, four-legged jacket-type offshore structures with different layers are generated in the software. Layer numbers are determined as 3, 4, 5, and 6. The structures modeled using the Lagrangian approach and the marine environment simulated through the Eulerian technique are depicted in Figure 1.a. B, b, and d indicate the base, the base side lengths, and the water depth, respectively. Perspective view of a six-layer structure and its environment are shown in Figure 1. a. On the other hand, the distribution of the layers of the structural models is presented in Figure 1. b. In this figure, h_1, h_2, h_3, and h_4 represent the height of the layers for each model. Wave and wind loads are defined as environmental conditions in the analyses. Since the water depth is constant in all models, the effect points of the wave and wind forces differ according to the models.

Figure 1: Coupled model and dimensions.

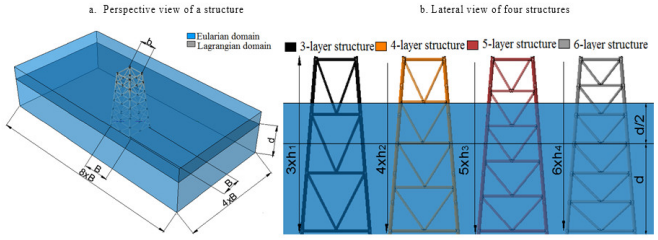

Source: Authors.

2.1. Structural Models.

Jackets typically consist of corner legs, fixed to the seabed, interconnected with horizontal and diagonal bracings. The base dimensions of all structural models (BxB) are 27 m × 27 m as shown in Figure 1. a. On the other hand, the top dimensions are 16 m × 16 m. The structures are modeled using structural steel material with Young's modulus of $2.1x10^{11}N/m^2$. Poisson's ratio is assumed to be 0.3 and the density value is taken as 7850 kg/m^3. On the other hand, the total mass of the platform is $1.50x10^5$ kg for all structures. Non-structural masses are defined as concentrated masses and symmetrically located at four corner nodes. Layer levels are equal in each relevant structure and the values are h_1=20 m, h_2=15 m, h_3=12 m, and h_4=10 m for 3, 4, 5, and 6 layer structures respectively. So, the total height of the structures is 60 m. The classification of the cases according to structural models is given in Table 1. D and e represent the diameter and thickness of the sections. L and m subscripts indicate leg and other members respectively. A total of 12 structural cases (SC) are determined by considering 3 different section sets for the structures having 4 different layer levels.

Table 1: Description of the structural cases.

Section properties (m) / Layer numbers	D_L=1,40 / e_L=0.014 D_m=1,00 / e_m=0.010	D_L=1,20 / e_L=0.012 D_m=1,00 / e_m=0.010	D_L=1,00 / e_L=0.010 D_m=0,80 / e_m=0.008
3	SC-1	SC-2	SC-3
4	SC-4	SC-5	SC-6
5	SC-7	SC-8	SC-9
6	SC-10	SC-11	SC-12

Source: Authors.

2.2. Environmental conditions.

The evaluated structures are taken into consideration for the combination of dead, wind, and wave loads. All structures serve at a depth of water of 30 m. The remaining 30 m part is in contact with the air. Wave forces affect structural members in contact with the marine environment. The other members that are in contact with air are affected by static wind forces. Hydrodynamic forces can be computed based on wave velocity (u) and acceleration (ú).

$$u = \frac{H}{2}\frac{gT}{L_W}\frac{\cosh[2\pi(y+d)/L_W]}{\cosh(2\pi d/L_W)}\cos(\frac{2\pi}{L_W}x - \frac{2\pi}{T}t) \qquad (1)$$

The velocity value derived from Eq. (1) is calculated based on wave theory, which relies on wave parameters including wave height (H), wave period (T), and water depth (d) at the location of the structure. Three environmental cases, including different H and T values as presented in Table 2 are used in the scope of the study.

Table 2: Description of the environmental cases.

Wave parameters	H=1.50 m	T= 8.00 s	H=2.00 m	T= 7.50 s	H=2.50 m	T= 6.00 s
Case name	EC-1		EC-2		EC-3	

Source: Authors.

The value of the wave length (L_w) in Eq. (1) is computed as 99.92 m, 87.82 m, and 56,20 respectively from cases 1 to 3 according to Linear Wave Theory. Wave velocity is designated as the input velocity for the analysis. Seawater is characterized as an EOS material with a density of 1025 kg/m^3, a dynamic viscosity of 1.50 x 10^{-3} Ns/m^2, and a sound velocity of 1560 m/s. Additionally, wind force constitutes another factor affecting elevation above the water surface (y).

$$u_a = \mathrm{U_{BAS}} k_T \ell n\,(y/z_0) \tag{2}$$

The environmental load impacting the structure is computed using Eq. (3) based on the Eurocode velocity profile (u_a) in any UBAS is the reference wind velocity (24 m/s), k_T symbolizes the terrain factor (0.17) and z_0 is the roughness length (0.01).

$$\mathrm{F}_a = \int_{\eta}^{L-\eta} \frac{1}{2} \rho_a u^2{}_{a(y)} C_s A_{(y)} dy \tag{3}$$

In Eq. (3), A represents the cross-sectional area of the member, ρa stands for the mass density of air, and Cs denotes the shape coefficient of the member, which is assumed to be 0.50 for cylindrical sections (Dyrbye and Hansen, 2004).

3. CEL Based FSI Analysis.

This section presents a bidirectional FSI analysis conducted through the CEL procedure using Abaqus. The analysis employs the conservation equations for mass, momentum, and energy within the framework of the Lagrangian approach.

$$\frac{D\rho}{Dt} + \rho \nabla \cdot v = 0 \tag{4}$$

$$\rho \frac{Dv}{Dt} = \nabla \cdot \sigma + \rho b \tag{5}$$

$$\frac{De}{Dt} = \sigma : D \tag{6}$$

In the equations, v, ρ, σ, b, and e represent material velocity, density, Cauchy stress, body force, and internal energy per unit volume, respectively. The conservation equations formulated for the Lagrangian approach are reassessed for the Eulerian approach through Eq. (6), resulting in the derivation of the generalized form given by Eq. (7).

$$\frac{D\varphi}{Dt} = \frac{\partial \varphi}{\partial t} + v \cdot (\nabla \varphi) \tag{7}$$

$$\frac{\partial \varphi}{\partial t} + \nabla \cdot \Phi = S \tag{8}$$

In the equations, φ, Φ and S are randomly assigned solution variables, flux function, and source term respectively. An explanation of the CEL technique is given in more detail in (Benson and Okazawa, 2004, Reddy, 2010). Structures and environments are instantiated based on the aforementioned mathematical definitions using Abaqus software. The modeling procedures are outlined as follows: The Eulerian section encompasses both material-assigned and unassigned (void) regions. The boundary conditions, along with the structural mesh configurations, are depicted in Figures 2-3 for the SC-1 case.

Figure 2: Boundary conditions.

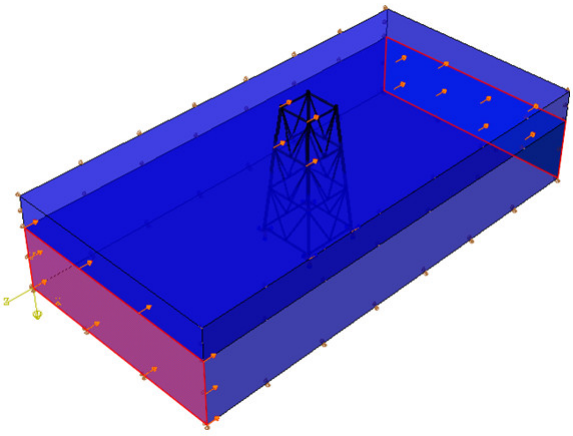

Source: Authors.

Figure 3: Mesh configuration.

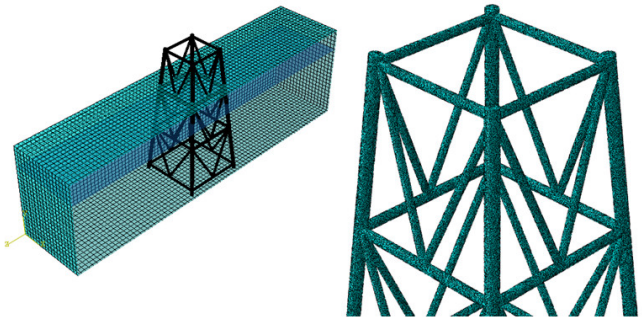

Source: Authors.

In Figure 2, the lower portion of the Eulerian domain is designated as an impermeable wall, the surfaces along the longer sides are designated as the far field, and the surfaces along the shorter sides are specified as the inlet and outlet boundaries. Eq. (1) is employed to determine the inlet velocity. Thus, the same parameters as the inlet surface are implemented to far fields. Wind forces affect the junction points of the second and third layers, as presented in Figure 2. N 347906 and 168405N are applied as wind load to the second and the third layers respectively for SC-1. Eq. (3) is used for the other structural cases and similarly calculated wind forces are affected by the junction points that contact with air. The mesh configuration of the finite element model is seen in Figure 3. The Lagrangian portion employs 4-node doubly curved elements for thin or thick shells, featuring reduced integration, hourglass control, and finite membrane strain (S4R) formulation. Furthermore, the Eulerian section utilizes 8-node linear brick elements, incorporating reduced integration and hourglass control (EC3D8R). Node spacings of 0.01 m and 0.25 m are considered for the Lagrangian and Eulerian components, respectively. The

number of nodes and elements that occur in the structural cases is given in Table 3.

Table 3: Node and element numbers of structural cases.

Structural case	Node number	Element Number	Structural case	Node number	Element Number
SC-1	13215533	12976821	SC-7	13312440	13076848
SC-2	13257727	13020107	SC-8	13329180	13092657
SC-3	13304897	13068412	SC-9	13228512	12990641
SC-4	13321048	13083847	SC-10	13272315	13035256
SC-5	13221680	12983303	SC-11	13320529	13086011
SC-6	13264750	13027298	SC-12	13338142	13102270

Source: Authors.

The equation of motion for the structure which is considered by finite elements program under external forces (F) can be written as follows.

$$m^{NJ}\ddot{X}^{N}|_{t} = \left(F^{J} - I^{J}\right)|_{t} \tag{9}$$

In Eq. (9); mNJ represents the mass matrix, FJ is the external applied load vector transferred from the Eulerian part, and IJ symbolizes the internal force vector caused by internal stresses of elements and acceleration. IJ is determined from the single elements such that a global stiffness matrix does not need to be constituted. Coupled Eulerian-Lagrangian analyses can be generated in Dynamic, Explicit steps only via the Explicit integration rule given by (ABAQUS User's Manual, 2015). Finite element analyses are conducted using a time step of 0.01 s, spanning a total duration of 64 s, equivalent to the eight-wave period of EC-1.

4. Results.

Finite element analyses are conducted with a time step of 0.01 s, covering a total duration of 64 s, corresponding to the eight-wave period of EC-1. Maximum displacement, reaction force, and Von-Mises stress values that are obtained from CEL analysis are given in Table 4.

Table 4: Maximum values of analysis results.

Structural cases	Environmental Cases								
	EC-1	EC-2	EC-3	EC-1	EC-2	EC-3	EC-1	EC-2	EC-3
	Displacement (m)			Reaction force (kN)			Stress (kN/m²)		
SC-1	0.85	0.71	0.98	127.36	120.97	142.55	933.15	870.40	1024.23
SC-2	1.07	0.91	1.15	117.02	110.91	136.90	806.44	713.11	932.11
SC-3	1.16	0.96	1.24	101.51	95.12	125.79	706.23	615.75	826.73
SC-4	0.70	0.63	0.84	105.21	105.03	132.04	851.62	745.50	957.68
SC-5	0.94	0.80	1.00	101.25	102.76	126.85	662.20	595.30	894.10
SC-6	1.02	0.89	1.12	93.47	84.26	101.18	610.40	543.33	714.60
SC-7	0.58	0.52	0.71	100.79	96.13	129.25	687.92	511.00	871.22
SC-8	0.76	0.66	0.82	94.55	86.22	121.81	570.56	422.11	746.26
SC-9	0.83	0.74	0.96	80.55	74.37	94.94	497.72	347.12	644.89
SC-10	0.51	0.46	0.64	94.18	92.23	120.73	508.13	406.34	828.33
SC-11	0.68	0.58	0.77	89.43	80.94	109.75	445.50	300.44	610.25
SC-12	0.77	0.65	0.85	77.13	69.84	86.03	335.71	260.28	497.63

Source: Authors.

Maximum displacement values vary between numerical models. While the difference is 12.94% between 6-layer and 5-layer models, it is obtained as 16.66 % between 5-layer and 4-layer models, and the variation is 10.71% between 4 and 3-layer models. Displacement distributions for each case where maximum displacement values occur are presented in Figure 4.

Figure 4: Displacement distributions of each case.

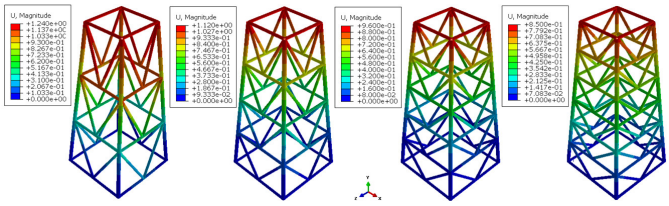

Source: Authors.

Maximum reaction force values are also compared between models. The differences are determined as 5.17%, 2.15%, and 7.95% between 6-layer and 5-layer models, 5-layer and 4-layer models, and 4-layer and 3-layer models, respectively. Finally, maximum Von-Mises values vary by 5.17% between 6-layer and 5-layer models, 9.92% between 5-layer and 4-layer models, and 6.94% between 4-layer and 3-layer models. Von-Mises stress distributions of the cases for the maximum values are given in Figure 5.

Figure 5: Stress distributions of each case.

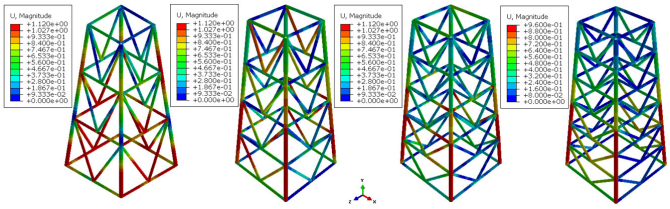

Source: Authors.

Coupled Eulerian and Lagrangian interaction for SC-1/EC-2, SC-4/EC-2, SC-8/EC-2, and SC-12/EC-2 are presented in descending order, in Figure 6. The movement of the water surface at different moments and the displacement of the structure depending on this movement can be seen in this way.

5. Machine Learning Analyses.

In this section, we evaluate the performance of three machine learning algorithms on the behavior of jacket-type offshore structures under different load effects. The dataset consists of 36 different jacket-type offshore structures under different conditions. The inputs are the layer number, wave load, leg diameter, and other member diameters. The outputs are displacement, reaction force, and stress values. Separate analyses are carried out for each of the outputs using machine learning techniques. Moreover, in order to assess how well one model performs in comparison to another, four metrics—R^2, RMSE, MAE, and MAPE—that are commonly employed are compared.

Figure 6: Coupling of Eulerian and Lagrangian domains.

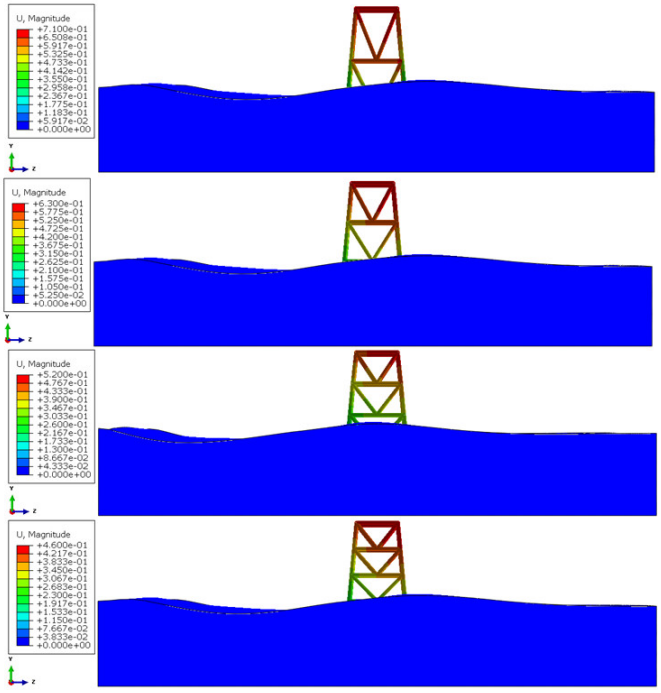

Source: Authors.

5.1. Prediction of Displacement Values.

An endeavor is made to estimate the displacement values of jacket-type offshore structures employing regression algorithms. In Table 5, the computed R^2 value of 0.97 indicates that the Xgboost regression model exhibits a high level of reliability and effectiveness in predicting the results of offshore structures. Additionally, the Xgboost technique exhibits lower RMSE, MAE, and MAPE values compared to other regression models, which confirms its efficacy in the estimation process.

Table 5: Performance metrics of regressors for testing data based on displacement output.

Model	R^2	RMSE	MAE	MAPE
XgBoost	0.97	0.03	0.02	0.03
Random Forest	0.86	0.06	0.05	0.06
Support Vector	0.79	0.08	0.06	0.07

Source: Authors.

The performance metrics of the regressors for the training data based on displacement output are shown in Table 6 for Xgboost, Random Forest, and Support Vector regressors. Upon evaluating the models on the training dataset, it is evident that all three regressors exhibit commendable performance, achieving accuracies above 95%. However, the Xgboost algorithm notably outperformed its counterparts, achieving a remarkable accuracy rate of 100%.

Table 6: Performance metrics of regressors for training data based on displacement output.

Model	R^2	RMSE	MAE	MAPE
XgBoost	1.00	0.01	0.01	0.01
Random Forest	0.97	0.04	0.03	0.04
Support Vector	0.94	0.24	0.18	0.45

Source: Authors.

Figure 7 shows the distributions of observed displacement versus the predicted displacement for the three regression models. The results reveal that all three machine learning algorithms yield improved fits concerning the training data and exhibit reduced variance in their forecasted values. Notably, Xgboost stands out as the most successful model among the three in this regard.

Figure 7: Dispersion of displacement values.

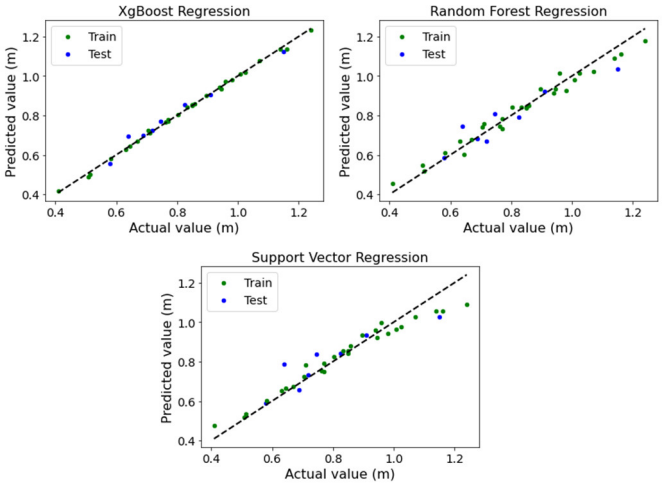

Source: Authors.

5.2. Prediction of Reaction Force Values.

The regression models are used to estimate the reaction force values of jacket-type offshore structures. We leverage four metrics to assess the performance of regression models. These include R^2, RMSE, MAE, and MSE. The performance metrics of the regression models based on the reaction force outputs for the testing data are shown in Table 7. After conducting a performance evaluation, the Random Forest model with an R^2 value of 0.94, RMSE of 5.67, MAE of 4.62, and MSE of 0.05 is ranked first in terms of performance metrics among the three models. It is followed by Support Vector and Xgboost regressors, respectively.

The performance metrics of the regression models based on the reaction force output of jacket-type offshore structure data can be seen in Table 8. Xgboost provides the best results when it comes to training data in comparison with the other two algorithms, as shown by a 95 % R^2 score. In addition, the Support Vector regressor exhibits underfitting behavior by having an R^2 score of 0.87 with the testing data, but only an R^2 score of 0.72 with the training data.

Table 7: Performance metrics of regressors for testing data based on reaction force output.

Model	R^2	RMSE	MAE	MAPE
XgBoost	0.85	8.91	7.26	0.08
Random Forest	0.94	5.67	4.62	0.05
Support Vector	0.87	8.39	7.43	0.07

Source: Authors.

Table 8: Performance metrics of regressors for training data based on reaction force output.

Model	R^2	RMSE	MAE	MAPE
XgBoost	0.98	3.83	2.82	0.03
Random Forest	0.94	6.24	4.29	0.05
Support Vector	0.72	0.52	0.27	1.77

Source: Authors.

The distributions of the observed reaction force vs. predicted reaction force of the three applied models are compared on the same graph in Figure 8. They are found to be in agreement, especially for the Xgboost and Random Forest models for training data. However, when evaluated in testing data, Xgboost had a slightly lower fit than the other models.

Figure 8: Dispersion of reaction force values.

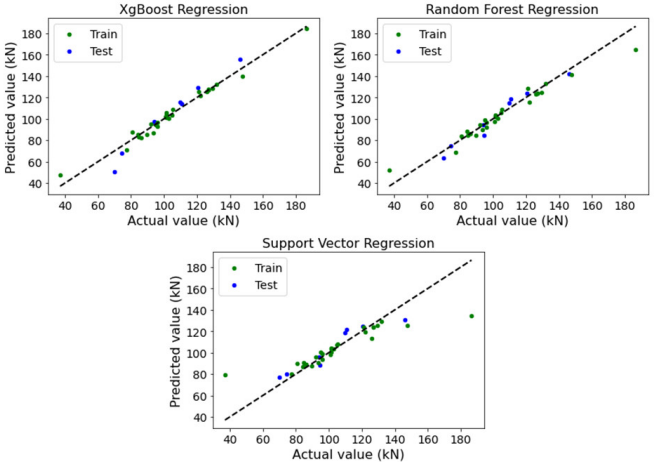

Source: Authors.

5.3. *Prediction of Stress Values.*

The performance of three machine learning algorithms is evaluated to find out their effectiveness in accurately predicting stress values of types of offshore structures. Table 9 displays the regression performance metrics for the test data based on the stress outputs. Xgboost outperforms other algorithms, having 0.92 R^2, 72.95 RMSE, 56.52 MAE, and 0.20 MAPE values. The performance of the Support vector regressor is the worst, with an accuracy of 0.80.

The regression performance metrics for the training data based on stress outputs are presented in Table 10. The results

Table 9: Performance metrics of regressors for testing data based on the output of stress value.

Model	R^2	RMSE	MAE	MAPE
XgBoost	0.92	72.95	56.52	0.20
Random Forest	0.82	107.75	94.71	0.29
Support Vector	0.80	115.52	81.73	0.34

Source: Authors.

show that three machine learning algorithms are all successful in predicting the stress value of training data. However, Xgboost performs better than the other two algorithms in terms of 100 % R^2.

Table 10: Performance metrics of regressors for training data based on stress value output.

Model	R^2	RMSE	MAE	MAPE
XgBoost	1.00	12.09	10.14	0.02
Random Forest	0.97	35.48	29.73	0.05
Support Vector	0.94	0.24	0.19	1.27

Source: Authors.

The distributions of the observed vs. predicted stress values of the testing and training data by three regressors are compared in Figure 9. The results show that Xgboost provides a better fit than all other models for both testing and training data, indicating that Xgboost can be used to predict the stress values of offshore jacket-type structures.

Figure 9: Dispersion of stress values.

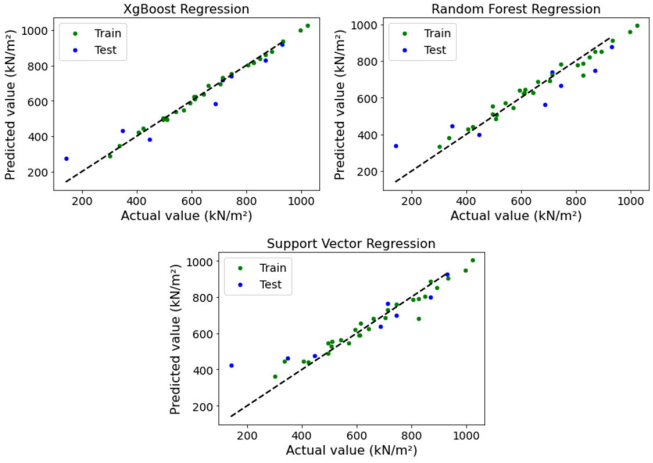

Source: Authors.

Conclusions.

The distributions of the observed vs. predicted stress values of the testing and training data by three regressors are compared in Figure 9. The results show that Xgboost provides a better fit than all other models for both testing and training data,

indicating that Xgboost can be used to predict the stress values of offshore jacket-type structures. Numerical analyses are widely used in structural designs and scientific studies with recent developments in computer technology. In this study, two different numeric analysis methods are used to investigate the behavior of the jacket-type offshore structures by considering the environmental loads. In the first part of the study, CEL-based FSI analyses are utilized. A total of 12 structural models are analyzed in 3 different marine environments. Displacement, reaction force, and stress values are determined for each structural case as presented in Table 4. While maximum values are obtained from EC-3 marine environment, minimum values are obtained from EC-2 marine environment for all structural models. In addition, maximum displacement values occur in models having the minimum diameter and wall thickness values for the same marine environment and layer number. On the other hand, maximum reaction force and stress values emerge in models with maximum diameter and wall thickness. Differences between models according to section, diameter, wall thickness, and layer properties for the same marine environment are presented proportionately in the Results section. It is seen that these rates remain lower than the rates realized in the change of section or marine environment according to Table 4. Consequently, it can be stated that the layer number has no significant effects on the examined outputs. The flow environment surrounding the structure is also obtained as well as the structural results. The structural displacement that changes because of the movement and free surface elevations of the wave at different time steps are seen in Figure 6. With the free water surface model, the effect of the wave motion on the unfluctuating water level on the structure has also been taken into consideration. The movement above the unfluctuating water level could be ignored in the case of CEL technique is not utilized. In the second phase of the investigation, predictive machine learning models are developed to assess the influence of layer number, wave load, leg diameter, and other member diameters on the displacement, reaction force, and stress performance of jacket-type offshore structures. Additionally, the performance of three distinct machine learning models concerning the behavior of jacket-type offshore structures under diverse load effects is evaluated.XGBoost demonstrates superior performance compared to Random Forest and Support Vector algorithms in predicting displacement and stress values. In contrast, Random Forest emerges as the most effective predictor for reaction force values. These findings indicate the promising potential for utilizing Xgboost and Random Forest in modeling the performance of offshore jacket-type structures. The present study contributes to the existing literature by employing machine learning algorithms to predict the performance of jacket-type offshore structures under different environmental load effects. Moreover, the research explores the reliability of machine learning predictions for forecasting purposes. It is crucial for future investigations to assess the accuracy of various machine learning algorithms and comprehend the parameters that influence their performance. Such endeavors will further enhance our understanding and utilization of machine-learning techniques in this domain.

References.

Zhang, P. et al. (2020) 'Bearing capacity and load transfer of brace topological in offshore wind turbine jacket structure', Ocean Engineering, 199. doi: 10.1016/j.oceaneng.2020.107037.

Xie, Y. et al. (2021) 'Experimental study on hydrodynamic characteristics of three truss-type legs of jack-up offshore platform', Ocean Engineering, 234. doi: 10.1016/j.oceaneng.2021-.109305.

Mousavi, Z. et al. (2023) 'Dictionary learning-based damage detection under varying environmental conditions using only vibration responses of numerical model and real intact State: Verification on an experimental offshore jacket model', Mechanical Systems and Signal Processing, 182. doi: 10.1016/j.ymssp.2022.109567.

Liu Y, Hajj M and Bao Y. (2022) 'Review of robot-based damage assessment for offshore wind turbines', Renewable and Sustainable Energy Reviews 158:112187. doi: 10.1016/j.rser.-2022.112187.

Lin JC, et al. (2022) 'Dilated generative adversarial networks for underwater image restoration', Journal of Marine Science and Engineering, 10:500. doi: 10.3390/jmse10040500.

Zhang, J. and Zhao, X. (2022) 'Wind farm wake modeling based on deep convolutional conditional generative adversarial network', Energy 238:121747.

Ferreira, C.A.S., et al. (2022) 'A framework for upscaling and modelling fluid flow for discrete fractures using conditional generative adversarial networks', Advances in Water Resources, 166:104264. doi: 10.1016/j.advwatres.2022.104264.

Oh, S. et al. (2021) 'Prediction of structural deformation of a deck plate using a GAN-based deep learning method', Ocean Engineering, 239:109835. doi: 10.1016/j.oceaneng.2021.1098-35.

Zhang, P. et al. (2020) 'Bearing capacity and load transfer of brace topological in offshore wind turbine jacket structure', Ocean Engineering, 199:107037. doi: 10.1016/j.oceaneng.20-20.107037.

Tran, T.T., Kim, E. and Lee, D. (2022) 'Development of a 3-legged jacket substructure for installation in the southwest offshore wind farm in South Korea', Ocean Engineering, 246:110-643. doi: 10.1016/j.oceaneng.2022.110643.

Tran, T.T. and Lee, D. (2022) 'Development of jacket substructure systems supporting 3MW offshore wind turbine for deep water sites in South Korea', International Journal of Naval Architecture and Ocean Engineering, 14:100451. doi: 10.1016-/j.ijnaoe.2022.100451.

Jalbi, S. and Bhattacharya, S. (2020) 'Concept design of jacket foundations for offshore wind turbines in 10 steps', Soil Dynamics and Earthquake Engineering, 139:106357. doi: 10.-1016/j.soildyn.2020.106357.

Wei, K., Myers, A. T. and Arwade, S. R. (2017) 'Dynamic effects in the response of offshore wind turbines supported by jackets under wave loading', Engineering Structures, 142:36–45. doi: 10.1016/j.engstruct.2017.03.074.

Chen, I.W. et al. (2016) 'Design and analysis of jacket substructures for offshore wind turbines, Energies, 9:264. doi: 10.3390/en9040264.

Bagheri. P. and Kim, J.M. (2019) 'Evaluation of cyclic and monotonic loading behavior of bucket foundations used for offshore wind turbines', Applied Ocean Research, 91:101865. doi: 10.1016/j.apor.2019.101865.

Abhinav, K.A. and Nilanjan, S. (2019) 'Nonlinear dynamical behaviour of jacket supported offshore wind turbines in loose sand', Marine Structures 57:133–151. doi: 10.1016/j.marstruc.2017.10.002.

Lu, H. et al. (2022) 'Rapid decoupling Laplace-domain algorithm for dynamic response estimation of offshore structures with asymmetric system matrices'. Ocean Engineering, 246:110534. doi: 10.1016/j.oceaneng.2022.110534.

Martínez, E.L. et al. (2009) 'Computational fluid dynamics simulation of the water – sugar cane bagasse suspension in pipe with internal static mixer', Computer Aided Chemical Engineering 26:683-688. doi: 10.1016/S1570-7946(09)70114-2.

Gücüyen, E., Erdem, R.T. and Gökkuş Ü (2016) 'FSI analysis of submarine outfall', Brodogradnja/Shipbilding, 67:67-80. doi: 10.21278/brod67205.

Korobenko, A. et al. (2017) 'FSI Simulation of two back-to-back wind turbines in atmospheric boundary layer flow', Computers and Fluids, 158:167-175. doi: 10.1016/j.compfluid.2017-.05.010.

Liu, J. (2016) 'A second-order changing-connectivity ALE scheme and its application to FSI with large convection of fluids and near contact of structures', Journal of Computational Physics 304:380–423. doi: 10.1016/j.jcp.2015.10.015.

Gücüyen, E. et al. (2020) 'Comparative analysis of tripod offshore structure', Gradevinar 72:1021-1030. doi: 10.14256/JCE.2848.2019.

ABAQUS User's Manual (2015) Version 6.12, SIMULIA, Dassault Systèmes Simulia Corp.

Khalilpourazari, S. et al. (2021) 'Designing energy-efficient high-precision multi-pass turning processes via robust optimization and artificial intelligence', Journal of Intelligent Manufacturing, 32:1621-1647. doi: 10.1007/s10845-020-01648-0. Khalilpourazari, S. and Pasandideh, S.H.R. (2021) 'Designing emergency flood evacuation plans using robust optimization and artificial intelligence', Journal of Combinatorial Optimization, 41:640–677. doi: 10.1007/s10878-021-00699-0.

Özyüksel, Ç.A. and Naser, M.Z. (2022) 'Hiding in plain sight: What can interpretable unsupervised machine learning and clustering analysis tell us about the fire behavior of reinforced concrete columns?', Structures, 40:920–935. doi: 10.10-16/j.istruc.2022.04.076.

Naser, M.Z. (2021) 'Mechanistically informed machine learning and artificial intelligence in fire engineering and sciences', Fire Technology 57:1–44, doi: 10.1007/s10694-020-01069-8.

Breiman, L. (2001) Random Forests. Machine Learning 45:5–32. doi: 10.1023/A:1010933404324

Chen, T. and Guestrin, C. (2016) 'XGBoost: A Scalable Tree Boosting System', Proceedings of the 22nd ACM SIGKDD International Conference on Knowledge Discovery and Data Mining. 785–794

Quinlan, J.R. (1986) 'Induction of decision trees', Machine Learning, 1, pp. 81–106. doi: 10.1007/BF00116251

Dyrbye, C. and Hansen, S.O. (2004) 'Wind loads on structures', John Wiley & Sons, Ltd. United Kingdom

Benson, D.J. and Okazawa, S. (2004) 'Contact in a multi-material Eulerian finite element formulation', Computer Methods in Applied Mechanics and Engineering, 193, pp. 4277-4298. doi: 10.1016/j.cma.2003.12.061

Reddy, J.N. (2010) 'Principles of continuum mechanics', Cambridge University Press. New York USA.